

Real-time hydro-environmental modeling and visualization system for public engagement

Joseph Hun-wei Lee · K. W. Choi

Received: 13 June 2008 / Accepted: 27 October 2008 / Published online: 5 November 2008
© Springer Science+Business Media B.V. 2008

Abstract Quantitative environmental impact assessment (EIA) provides a tool for decision makers and the public to understand issues relating to sustainable development. The use of advanced hydro-environmental modelling and visualization technology can help to provide an intuitive and interactive digital platform to better communicate EIA issues and thus promote continuous public involvement and stakeholder engagement. Such a platform must be based on a robust hydrodynamic model engine that provides seamless predictions from the near to far field. This lecture summarizes the key issues of impact assessment in urban coastal cities, and presents examples of impact assessment of several major sewage outfalls, including the Hong Kong Harbour Area Treatment Scheme. The predictions of a recently developed Distributed Entrainment Sink Approach (DESA) for dynamic coupling of the near and far fields are compared with alternative “actual source” approaches and field experiments. The conceptual elements of a real time water quality forecast and management system are outlined.

Keywords Mixing and transport · Environmental impact · Risk assessment · Public engagement · Three-dimensional models · Hydrodynamics and water quality

1 Introduction

Quantitative environmental impact assessment (EIA) plays an important role in the sustainable development of coastal and marine resources. In many urban metropolis, it is often necessary to predict the impact of development projects or pollution discharges and the associated environmental risks in a coastal water. And yet worldwide there is currently no robust

J. H.-W. Lee (✉) · K. W. Choi
Croucher Laboratory of Environmental Hydraulics, Department of Civil Engineering,
The University of Hong Kong, Pokfulam Road, Hong Kong, China
e-mail: hreclhw@hkucc.hku.hk

K. W. Choi
e-mail: chojdkw@hkucc.hku.hk

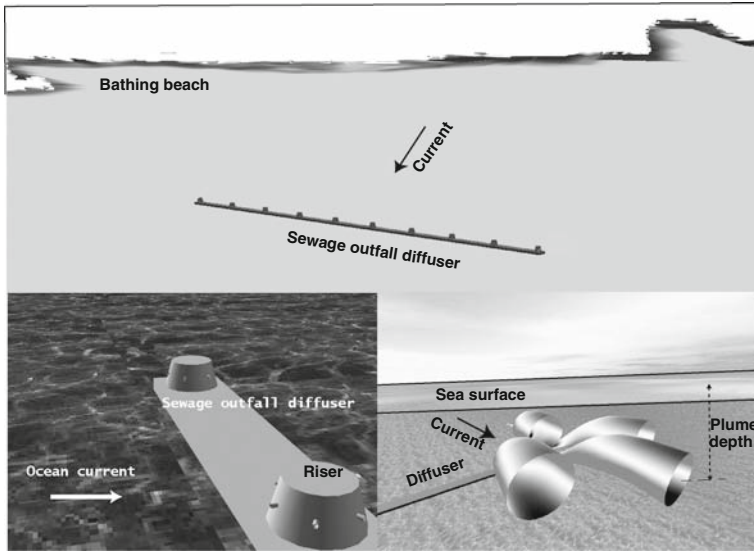


Fig. 1 Submarine sewage discharge depicted in virtual environment

model for satisfactory risk assessment and effective communication of the predicted impact to the stakeholders.

Traditionally, predictions of the environmental impact of various development scenarios (e.g. major bridge crossing, population growth, various degrees of sewage treatment) are mainly presented in the form of two-dimensional hard-copy plans. This type of presentation is not easily understood by non-technical stakeholders; the lack of effective communication tends to breed misunderstanding and mistrust, thus making meaningful dialogue between project proponents and the public stakeholders difficult. More recently, there has been a growing emphasis on the use of interactive 3D models to better communicate EIA issues and thus promote continuous public involvement and stakeholder engagement. With the use of the latest 3D modelling and visualization technology, the public would be able to visualize and better understand the impact of different scenarios and mitigation measures, and offer comments and suggestions in the project planning and implementation stages (<http://www.epd.gov.hk/eia/3deia>). A virtual reality tool for 3D EIA is depicted in Fig. 1. Such a system must be based on a robust hydrodynamic engine.

Despite advances in hydrodynamic and water quality modelling, current methods of impact assessment have several limitations. First, for environmental risk assessment it is necessary to predict the impact of effluent discharges for a wide spectrum of discharge and ambient conditions. The mixing of buoyant jets into a stratified co-flowing, cross-flowing, and counter-flowing current, with three-dimensional jet trajectories, has to be modelled. However, near field plume models typically can cater for only limited scenarios (e.g. jets with 2D trajectories); hence a comprehensive statistical risk assessment cannot be carried out. Second, for many densely populated coastal cities in Asia Pacific countries, the effluent discharges are typically located in relatively shallow waters of 5–20 m depth, close to sensitive receivers such as beaches or fisheries. This necessitates the accurate prediction of pollutant concentrations over a wide spectrum of length scales, from several meters (e.g. benthic impacts) to several kilometres. Impact assessment tools must be able to cater for both the near field and

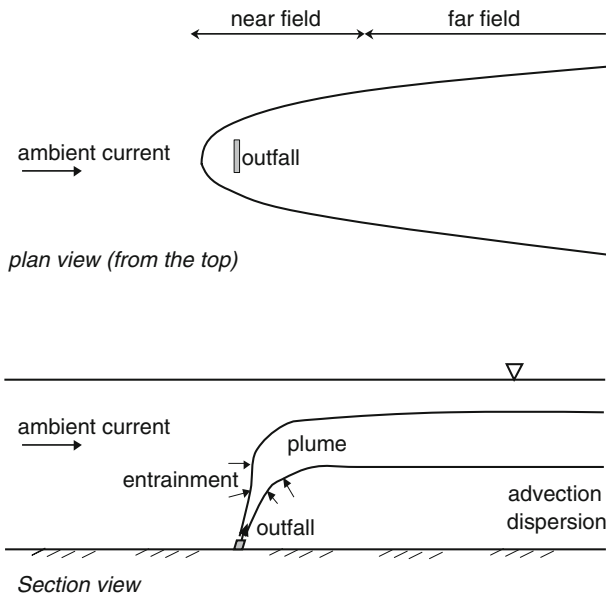


Fig. 2 Mixing and transport of submerged effluent discharge

the far field. Currently industry-standard models typically cater for only the near field or only the far field.

Near field models give predictions of pollutant concentrations in the initial mixing zone, a region of the order of several water depths from the source. While turbulent plume entrainment is properly modelled, important initial mixing characteristics such as the gravitational spreading layer and its coupling with plume entrainment cannot be predicted by such integral type jet models. On the other hand, 3D shallow water circulation models are run on grids in the order of 100 m. Predictions tend to be overly optimistic as the impact is averaged over a region at least of the order of 100 m. And yet, predictions are often needed in the transition from the near to far field, or the intermediate field (Fig. 2). For example, the impact of a chlorinated wastewater discharge on a nearby beach located 3 km down current needs to be assessed. In general, the use of either the near field model or the far field model alone is highly unsatisfactory. All the existing near-far field coupling methods involve either “one-way coupling” or weakly “two-way coupling”; hence the dynamic effects of the plume mixing are not satisfactorily represented in the far field model [16,5,1].

This paper describes the core of a GIS-based and integrated hydraulic-virtual reality (VR) system that enables effective impact and risk assessment. First, a new Distributed Entrainment Sink Approach (DESA) for the dynamic coupling of the near and far field is described. The DESA method [2] enables seamless 3D environmental impact prediction from the near field to the far field; the robust method also enables practical computations for statistical risk assessment. Second, the advantages of the method over alternative “actual source” methods are demonstrated for several prototype sewage outfalls. Finally, model predictions of plume mixing in the intermediate field are compared with field data for an outfall in British Columbia, Canada. The basic elements of a real time water quality forecast and management system are briefly outlined.

2 Near and far field coupling

The mixing and transport in the intermediate field (Fig. 2) can be predicted by dynamic near-far field coupling using a recently developed Distributed Entrainment Sink Approach (DESA) [2]. The Environmental Fluid Dynamics Code (EFDC) based on two-equation turbulence closure is adopted as the 3D shallow water circulation model [4]. A well-validated Lagrangian model (JETLAG) is used as the near field plume model ([7,9]). The effect of the plume mixing on the surrounding flow is modelled by a distribution of sinks along the plume trajectory and an equivalent diluted source flow at the predicted terminal height of rise. A two-way dynamic link can be established at *grid cell* level between the near and far field models. The coupling captures the key physical mechanisms of (i) turbulent jet entrainment; and (ii) 3D hydrodynamics with hydrostatic pressure approximation in the intermediate field.

In this coupling method, at any time instant t_k , the ambient current $U_a(z)$, salinity $S_a(z)$, temperature $T_a(z)$, density $\rho_a(z)$, and tracer concentration $C_a(z)$ upstream of the outfall discharge is provided by the solution at the grid cells upstream of the source. Based on the ambient conditions, the embedded Lagrangian jet model JETLAG is run to compute the evolution of the average properties of the Lagrangian plume elements along the jet trajectory: average jet velocity and width, tracer concentration, location, density, and the total fluid mass entrained into the plume element as a result of shear and vortex entrainment, ΔM_k . Based on the location of the centre of the plume elements, the distributed entrainment sinks, Q^e , for each far field model grid cell can then be computed by summing the entrainment flows corresponding to all the plume elements within that cell:

$$Q^e = \sum \left(\frac{\Delta M_k}{\rho_a \Delta t} \right) \quad (1)$$

The diluted source flow at terminal height of rise, Q^d , is then given by:

$$Q^d = Q_o + \sum Q^e \quad (2)$$

and applied as a source term to the corresponding far field model grid cell, where Q_o is the effluent discharge flow. Also, a source term representing the discharged pollution loading (tracer mass flux) is introduced at the terminal height of rise (i.e. the near field mixing is represented as fluid mass source in the continuity equation and tracer mass source in the tracer transport equation). The governing equations of the 3D hydrodynamic model are then solved to obtain an updated solution on the 3D far field grid. The dynamic linkage is illustrated in Fig. 3. More details can be found in Choi and Lee [2].

Unlike alternative approaches, the dynamic coupling at grid cell level (along the entire time-dependent jet trajectory) ensures that the near field mixing is fully embedded into the 3D far field model in an essentially grid-independent manner. Unsteady tidal situations can be readily modeled, and there is no need to specify parameters such as the size of mixing zone or layer thickness. Full mass conservation is achieved at cell-level for the entire grid. The DESA method has been tested against basic experimental data of a variety of complex flows including buoyant plumes in stagnant, flowing and stratified environments. The numerical predictions are in excellent agreement with experimental data [2]. To facilitate public engagement, a virtual reality, PC-based version of the near field model, VISJET, has also been developed [8,9]. Figure 4 shows a VISJET simulation of the near field jet mixing of rosette risers mounted on a submerged ocean outfall; on each riser an 8-jet group discharges the effluent in the form of a rosette. Figure 5 shows a comparison of the predicted and observed buoyant surface layer in the intermediate field of a laboratory rosette jet group [6].

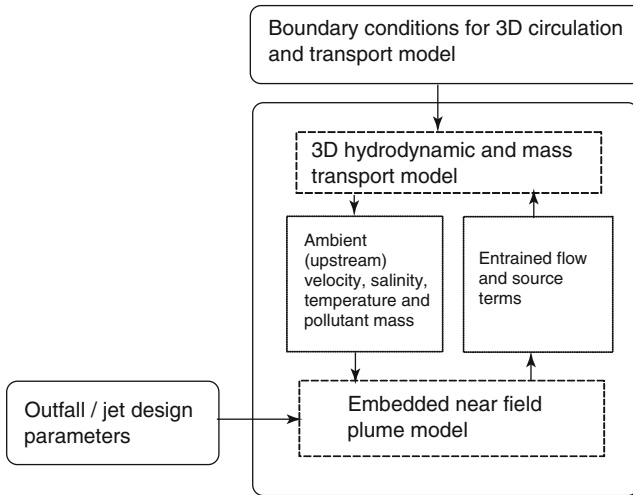


Fig. 3 Dynamic coupling of near- and far-field model for simulating environmental discharge

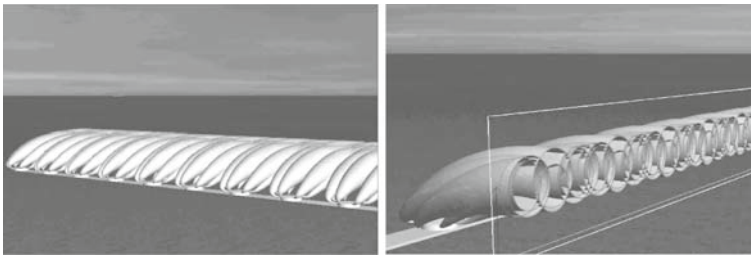


Fig. 4 VISJET Simulation of eight jet group in nonlinear-stratified water

As an alternative to dynamic coupling, an “actual source” (AS) approach can also be used (e.g. [16, 14])—i.e. the source flow and pollutant mass are introduced into the grid cell(s) which contain the actual outfall. By the nature of the purely far field approach, the AS method cannot account for the plume rise due to vertical jet momentum; it is shown to predict exaggerated mixing, and hence a much lower trapping level than experimental observations [2, 3]. Without a sub-grid near field model, the AS method also gives results that are strongly grid dependent.

3 Impact assessment of prototype sewage outfall discharges

3.1 Mixing and transport of outfall discharges

The need and importance of a robust and accurate near-far field coupling method is illustrated using the following numerical simulations. The DESA approach is applied to predict the impact of the Hong Kong Harbour Area Treatment Scheme (HATS). A sewage flow of around 1.4 million m³/d is centrally collected from both sides of the Victoria Harbour through a tunnelled sewerage system and receives Chemically Enhanced Primary Treatment (CEPT) at Stonecutters Island. CEPT removes about 70% of the organics, 80% of suspended solids,

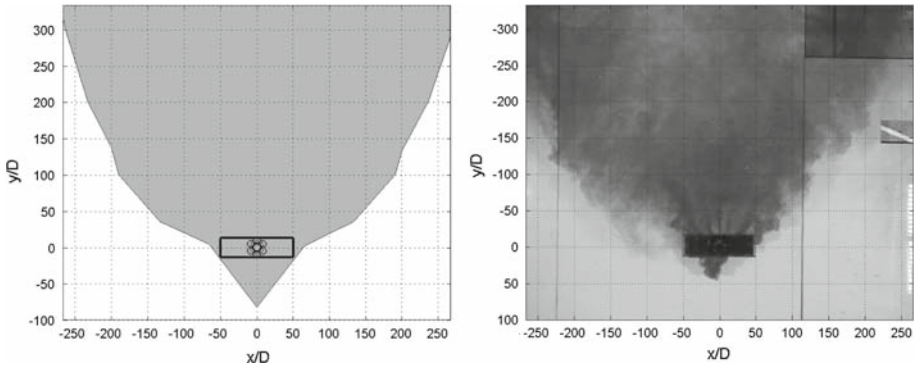


Fig. 5 Comparison of the predicted buoyant surface layer with experiments (6 jets, $Fr=15$, $U_a = 3$ cm/s, $H=0.3$ m and $D=0.3$ cm)

Table 1 Discharge and ambient parameters for prototype outfall cases

	Discharge rate Q (m^3/s)	Diffuser length L (m)	Water depth H (m)	Initial density difference $\Delta\rho/\rho_a$	Vertical density gradient $d\rho_a/dz$ (kg/m^4)
HK outfall 1	18.0	1200	12.0	0.01177	2.36×10^{-4}
HK outfall 2	23.7	1200	22.0	0.01645	3.36×10^{-4}
Boston	20.0	2000	30.0	0.01674	1.15×10^{-4}
Lions Gate	1.0	42.7	22.0	0.02253	Measured profile

and 50% of bacteria. The CEPT effluent is discharged through a 1.2km long submerged outfall diffuser into the harbour at a dry weather flow of $18\text{ m}^3/s$. The effluent is discharged through 24 “rosette” risers, at a mean depth of around 12 m. Each riser has 8 discharge ports (HK outfall 1 in Table 1). For comparison over the typical range of operating conditions, the impact of a similar diffuser (with 12 rosette risers and 6-jet groups) at an alternative site of depth 22 m (Hong Kong outfall 2) is also studied along with the Boston Sewage outfall [14]. The key parameters for the three outfalls are listed in Table 1.

The impact of the effluent discharge in the vicinity of the outfall is illustrated for a schematized situation. A computational domain of 10km by 10km is considered, and a model grid of $40 \times 40 \times 10$ is employed. Based on field data, a linear ambient density stratification is applied. Simulations are performed for different constant ambient velocities. The HATS outfall is represented by 5 equivalent risers over the same diffuser length, each with 8 ports of diameter 57.7 cm; whilst maintaining the same flow, momentum and buoyancy flux per unit length of diffuser. Each of the 8 jets in the rosette jet group (with 3D jet trajectories) can be readily predicted by JETLAG to furnish the source terms for the far field model. The solution of the flow and tracer concentration field can then be obtained. Under summer stratification conditions, the effluent is typically trapped beneath the free surface; the mixed effluent is hence advected in a layer that is shielded from solar radiation. The trapping level is of concern as bacterial decay is sensitive to light extinction and travel times to sensitive receivers [12]. The minimum dilution can then be obtained from the maximum concentration at the trapping level. Figure 6 shows the predicted minimum dilution S_m (inverse of maximum

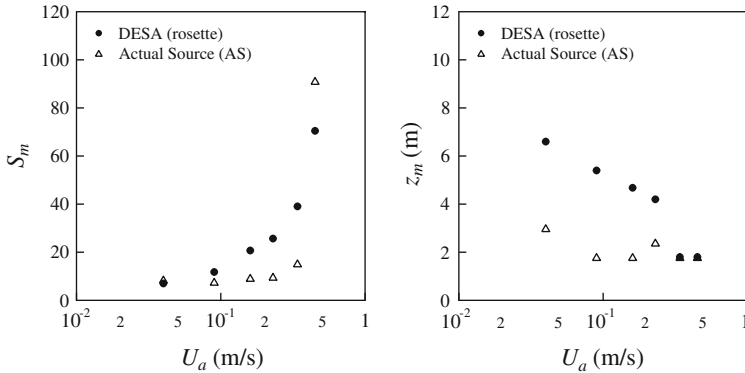


Fig. 6 Predicted minimum dilution and trapping level of the Hong Kong (HATS) outfall discharge in a stratified crossflow

relative concentration) and the trapping level z_m as a function of the ambient current speed. The results using the AS method are also shown as a comparison; the source terms are added to 5 grid cells at the bottom. It can be seen that as the ambient current increases, the dilution increases resulting in a decreased trapping level (i.e. sewage field trapped closer to bottom). The “actual source” approach predicts the same trend; however, the trapped level is lower and the dilution is less; in addition both S_m and z_m are not quite sensitive to the ambient current over a certain range. Analysis of the computed concentration distribution in a vertical section of the plane of symmetry (not shown) shows that the AS method results in a lower trapped layer with higher concentrations.

The protection of beach water quality is a major issue in many countries, and impact assessments and beach closures are often based on predicted bacteria concentrations in terms of *E. coli*. Figure 7 shows the time variation of the predicted *E. coli* concentration at the trapping level at a distance 2 km downstream of the source. The bacterial mortality is based on the Mancini [12] approach:

$$k = (k_b + k_s S) \theta_T^{T-20} + k_I I \left(\frac{1 - e^{-e_t H}}{e_t H} \right) e^{-e_t d} \tag{3}$$

where k = first order bacterial mortality rate (d^{-1}), k_b = basic mortality rate (d^{-1}), k_s = salinity related coefficient ($\text{ppt}^{-1} d^{-1}$), S = salinity (ppt), θ_T = temperature coefficient, T = temperature ($^{\circ}C$), k_I = radiation related coefficient ($\text{m}^2 \text{W}^{-1} d^{-1}$), I = daily solar UV-radiation at the water surface (Wm^{-2}), e_t = extinction coefficient (m^{-1}), H = water depth (m) and d = water level below surface (m), respectively. It can be seen that the AS approach tends to under-predict bacteria concentrations by a factor of 2–3. In addition, the effect of a variable bacteria decay coefficient (due to vertical light attenuation and changing salinity) is also shown; the use of a constant mortality rate tends to give optimistic impact assessments. Finally, Fig. 8 shows a plot of the computed dimensionless minimum dilution $(S_m q N)/b^{2/3}$ and trapping level z_m/l_b as a function of the crossflow Froude number $F = U_a^3/b$ for all the three prototype outfalls, where q, b = volume and buoyancy flux per unit diffuser length (see Table 1), $N = \sqrt{-(g/\rho_a)(d\rho_a/dz)}$ is the buoyancy frequency, and $l_b = b^{1/3}/N$ is a stratification length scale. Consistent with experimental observations [13], there is a clear increasing trend for the dilution predicted by DESA with F , while the predicted dilution by AS remains in

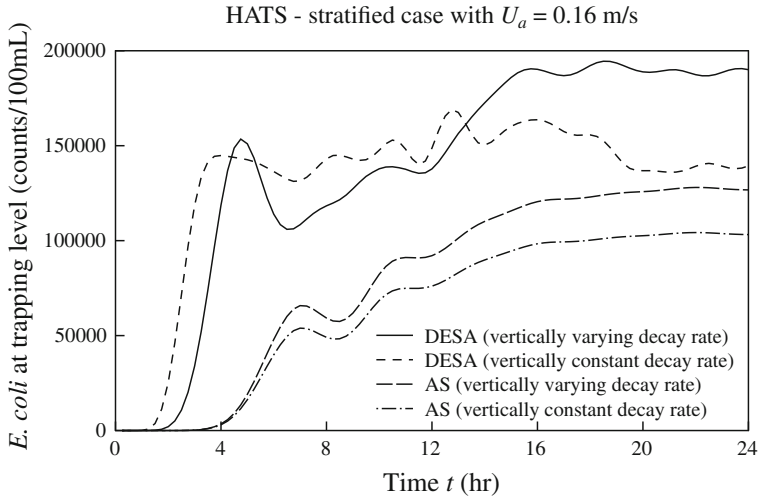


Fig. 7 Computed *E. coli* concentration at the trapping level 2 km downstream of the Hong Kong (HATS) outfall discharge in stratified crossflow ($U_a = 0.16$ m/s)

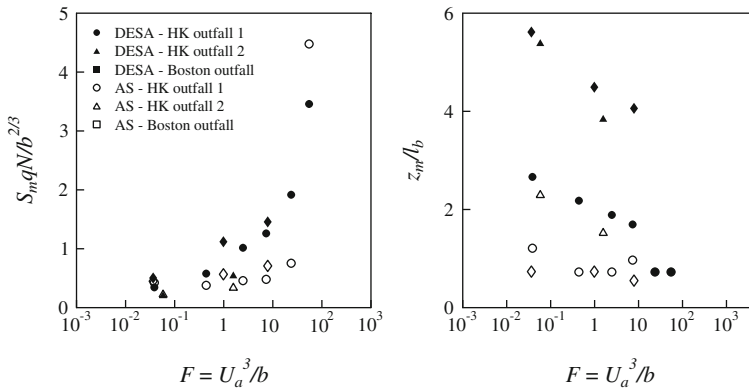


Fig. 8 Dimensionless minimum dilution and trapping level of three prototype sewage outfalls in stratified crossflow

a very narrow range except for a case with strong current when a trapped layer along the bottom is formed.

3.2 Risk assessment of environmental discharges

The impact of the HATS outfall at Stonecutters Island has also been simulated using DESA on a full 3D model of the entire Hong Kong waters. A boundary-fitted curvilinear horizontal grid covering the entire Hong Kong Waters is used. It has 10,146 active cells in the horizontal plan with 8 vertical σ -layers and a grid size of 200–300 m near the outfall. Typical wet and dry season conditions with constant freshwater runoff from the Pearl River are considered. Each numerical simulation covers a 15-day Spring-Neap tidal cycle. The environmental risk of a sewage outfall discharge can be assessed using an integrated stochastic (Monte-Carlo) method that couples the 3D hydraulic and mass transport model with the species sensitivity

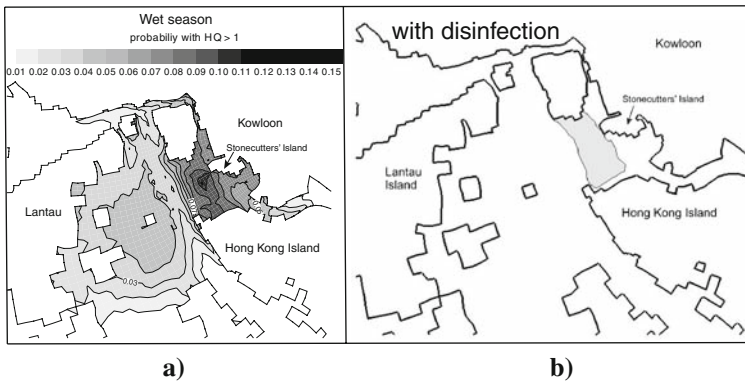


Fig. 9 **a** Spatial distribution for computed probability with hazard quotient >1 for HATS discharge for wet season and **b** Mixing zones based on the 95 percentile of predicted surface *E. coli* concentrations for HATS Stage 2A flow in wet season with disinfection

distribution (SSD), a cumulative probability distribution describing the variation of sensitivity towards a target toxic pollutant among a set of species. The risk can be quantified in term of hazard quotient ($HQ = EC/BC$), the ratio between the environmental exposure concentration (EC) and toxic threshold effects levels (BC); $HQ > 1$ indicates risky harmful effects on the environment due to the target pollutant. In connection with HATS outfall, unionised ammonia is the target pollutant that is toxic to marine life. The 3D simulations produce time series of unionised NH_3-N concentrations at desired time interval for every far field grid cell, which can be used to obtain the corresponding probability function for the environment concentration (EC). With the benchmark concentration (BC) randomly sampled from the Species Sensitive Distribution for NH_3-N , an ensemble of hazard quotient ($HQ = EC/BC$) can be generated for determining the probability density and cumulative probability distribution of HQ at each grid cell. The spatial variation of environmental risks in terms of HQ can hence be examined and corresponding risk maps can be produced (Fig. 9a). Such a comprehensive statistical risk assessment is found to be less sensitive to arbitrary definitions of prescribed threshold toxicity levels, and can only be made with a robust hydro-environmental modelling engine.

3.3 Field validation: Lions gate outfall, British Columbia

Li and Hodgins [10] reported results of dye tracing field experiments for the Lions Gate Wastewater outfall, British Columbia, Canada. The Lions Gate wastewater treatment plant outfall discharges primarily treated effluent into a well-flushed tidal channel (Burrad Inlet). The sewage is discharged through a 42 m long outfall diffuser (with 10 ports) on the sea bed where the depth is around 22 m, at a narrow section of the channel (500 m wide), in observed tidal currents of 0.1–0.6 m/s. As the interest is mainly in the mixing and transport in the intermediate field, and the characteristics of the trapped sewage field, numerical computations can be made on a schematized rectangular channel of 500 m width and 22 m depth, with a uniform crossflow corresponding to the observed current speeds of 0.1–0.6 m/s; the field observed ambient density profile and sewage flows are used. A constant discharge rate of $1 \text{ m}^3/\text{s}$ and source tracer concentration of 1,000 ppb are adopted in all the simulated cases. A computational grid of $40 \times 19 \times 10$, with uniform grid size of 25 m by 25 m is employed. As discussed previously, the effluent discharge is represented by a number of equivalent

Table 2 Comparison between predicted and observed trapping depths and dilutions for Lions Gate Outfall, British Columbia, Canada

Predicted by DESA			Observed [11]		
Ambient current (m/s)	Dilution (C_0/C)	Trapping depth (m)	Ambient current (m/s)	Dilution (C_0/C)	Trapping depth (m)
0.1	12.0	7.7			
0.2	38.3	11.0			
0.3	75.2	12.5	0.1–0.6	8–25	9.5–14
0.4	153.8	14.0			
0.5	158.7	14.3			

non-interfering jets, maintaining the same volume, buoyancy and momentum fluxes per unit diffuser length. The trapping depth (location of trapping level below free surface) d_m and the dilution (inverse of maximum concentration) C_0 can be obtained from the DESA solution of the tracer concentration field for different currents (Table 2). The dynamically coupled model predicts a trapping depth of 7.7–14.3 m, while the field observations indicate a corresponding range of 9.5–14 m. In addition, the predicted dilution at trapped depth ranges from 12–38 for $U_a = 0.1$ –0.2 m/s compares favorably with the observed values of 8–25 (measurements carried out shortly after tidal slack). Knowledge of the detailed topography and exact tidal harmonics for the area are expected to further refine the predictions.

4 Concluding remarks

A robust pilot hydro-environmental modelling and visualization system has been developed for environmental impact assessment and public engagement. The hydraulic and water quality prediction rests on a recently developed method of dynamic coupling of the near and far field, giving seamless predictions and enabling practical computations of statistical risk assessment. The system is equipped with an intuitive user interface, and allows (i) 3D virtual reality; (ii) terrain and scene modelling (e.g. bridges, beaches, power stations); and (iii) flow visualization over the Internet. Sample videos of the 3D EIA for Hong Kong waters can be downloaded from <http://www.aoe-water.hku.hk/visjet>.

The system facilitates effective public engagement in several ways: (a) The seamless prediction from the near to far field enables the proper definition of mixing zones—often defined to be the region within which the water quality standard may be exceeded. Figure 9b shows the mixing zone of the HATS scheme with respect to the surface *E.coli* concentration ($\leq 180/100$ ml) during the wet season (with disinfection). The ability to determine mixing zones can reduce many potential disputes that often arise due to unclear definition. (b) The system allows the user to navigate through the region of interest and view the impact from different perspectives. This gives a much better sense of realism of the environmental impact. Most importantly, the system allows interactive interrogation; the user can ask for information on concentration at any given location, composite dilution of jet groups and sewage layer thickness at any cut-plane, or pose what-if questions (e.g. change in discharge location). (c) As an example scenario, the sewage plant in a town is to be upgraded to cater for population growth. The sewage is to be discharged after treatment into the adjacent sea through a submerged outfall diffuser. A key stakeholder group, the local fishermen, is concerned that

the increase in sewage (freshwater) discharge will result in decrease of salinity and affect the fisheries yield. The system can be readily used to demonstrate: (i) the spatial and temporal extent of the impact; (ii) the change in salinity at any location; (iii) the increase of *E. coli* concentration in the nearby beach—all against a realistic GIS background. (d) With a better appreciation of the problem, the local stakeholders can provide useful feedback and may offer suggestions on possible improvements—e.g. alternative discharge locations, or optimisation of disinfection dosages at different times of the day. This 3D EIA system forms the basis of a real time water quality forecast and management system for Hong Kong (WATERMAN). The EIA predictions can be integrated with predictions of likelihood of red tides and algal blooms [15] and beach water quality forecasts, for the benefit of the public.

Acknowledgements This work is supported by the Hong Kong Research Grants Council (Project No. HKU 7518/03), and in part by a grant from the University Grants Committee (Project No. AoE/P-04/04).

References

1. Bleninger T, Jirka GH (2004) Near- and far-field model coupling methodology for wastewater discharges. In: Lee JHW, Lam KM (eds) Environmental hydraulics and sustainable water management. Taylor & Francis, London pp 447–453
2. Choi KW, Lee JHW (2007) Distributed entrainment sink approach for modelling mixing and transport in intermediate field. *J Hydraul Eng, ASCE* 133(7):804–815
3. Choi KW, Lee JHW (2007) Reply to Discussion of “Distributed entrainment sink approach for modelling mixing and transport in the intermediate field”. *J Hydraul Eng, ASCE* 134 (December 2008, in press).
4. Hamrick JM (1992) A three-dimensional environmental fluid dynamics computer code: theoretical and computational aspects. The College of William and Mary, Virginia Institute of Marine Science, Special Report 317, 63 pp
5. Kim YD, Seo IW, Kang SW, Oh BC (2002) Jet integral—particle tracking hybrid model for single buoyant jets. *J Hydraul Eng, ASCE* 128:753–760
6. Lai ACH, Yu D, Lee JHW (2007) Near and intermediate field mixing of a rosette jet group. Proceedings of the fifth international symposium on environmental hydraulics, Tempe, Arizona, USA (CD-ROM), 4–7 December 2007
7. Lee JHW, Cheung V (1990) Generalized Lagrangian model for buoyant jets in current. *J Environ Eng, ASCE* 116(6):1085–1105
8. Lee JHW, Cheung V, Wang WP, Cheung SKB (2000) Lagrangian modeling and visualization of rosette outfall plumes. Proceedings of the hydroinformatics 2000, Iowa (CDROM), 23–27 July 2000
9. Lee JHW, Chu V (2003) Turbulent jets and plumes—a Lagrangian approach. Kluwer Academic Publishers, 390 pp
10. Li S, Hodgins DO (2004) A dynamically coupled outfall plume-circulation DO model for effluent dispersion in Burrard Inlet, British Columbia. *J Environ Eng Sci* 3:433–449
11. Li S, Hodgins DO (2008) Field and numerical investigation of the fate and effects of wastewater discharges into coastal waters. Proceedings of the international conference on waste engineering and management, Hong Kong, 28–30 May
12. Mancini JL (1978) Numerical estimates of coliform mortality rates under various conditions. *J WPCF* 50:2477–2484
13. Roberts PJW, Snyder WH, Baumgartner DJ (1989) Ocean outfalls, I: submerged wastefield formation. *J Hydraul Eng, ASCE* 115(1):1–25
14. Signell R P, Jenter H L, Blumberg A F (2000) Predicting the physical effects of relocating Boston’s Sewage Outfall. *Estuar Coast Shelf Sci* 50:59–72
15. Wong KTM, Lee JHW, Hodgkiss IJ (2007) A simple model for forecast of coastal algal blooms. *Estuar Coast Shelf Sci* 74:175–196
16. Zhang XY, Adams EE (1999) Prediction of near field plume characteristics using far field circulation model. *J Hydraul Eng, ASCE* 125(3):233–241